Review Article

Pulmonary vasculitis: diagnosis and endovascular therapy

Kiran Batra[1], Murthy Chamarthy[1], Rodrigo Caruso Chate[2], Kirk Jordan[1], Fernando Uliana Kay[1]

[1]UT Southwestern Medical Center, Dallas, TX, USA; [2]Hospital Israelita Albert Einstein and Instituto to Coração HCFMUSP, Sao Paulo, Brazil

Contributions: (I) Conception and design: K Batra, FU Kay; (II) Administrative support: K Batra, FU Kay; (III) Provision of study material or patients: K Batra, M Chamarthy, K Jordan, RC Chate; (IV) Collection and assembly of data: All authors; (V) Data analysis and interpretation: All authors; (VI) Manuscript writing: All authors; (VII) Final approval of manuscript: All authors.

Correspondence to: Fernando Uliana Kay, MD. UT Southwestern Medical Center, Dallas, TX, USA. Email: fernando.kay@utsouthwestern.edu.

Abstract: Pulmonary vasculitides are caused by a heterogeneous group of diseases with different clinical features and etiologies. Radiologic manifestations depend on the predominant type of vessel involved, which are grouped into large, medium, or small-sized vessels. Diagnosing pulmonary vasculitides is a challenging task, and radiologists play an important role in their management by providing supportive evidence for diagnosis and opportunities for minimally invasive therapy. This paper aims to present a practical approach for understanding the vasculitides that can affect the pulmonary vessels and lungs. We will describe and illustrate the main radiologic findings, discussing opportunities for minimally invasive treatment.

Keywords: Computed tomography (CT); angiography; radiography; vasculitis; magnetic resonance

Submitted Nov 16, 2017. Accepted for publication Dec 04, 2017.
doi: 10.21037/cdt.2017.12.06
View this article at: http://dx.doi.org/10.21037/cdt.2017.12.06

Introduction

Vasculitides comprise a heterogeneous group of diseases characterized by inflammation and damage to vessels in multiple organs and systems (1-3). A nomenclature system for classifying systemic vasculitides was proposed after the first International Chapel Hill Consensus Conference in 1994 (4), and revised during the second consensus conference in 2012 (5). The classification system attempts to group entities based on the predominant type of vessels affected (*Figure 1*), i.e., large (aorta, main branches and analogous veins), medium (main visceral arteries, veins, and initial branches), or small-sized vessels (intraparenchymal arteries, arterioles, capillaries, venules and veins). Additional features used to characterize different vasculitides include etiology, pathogenesis, type of vessel affected, type of inflammatory infiltrate, organ distribution, clinical presentation, genetic link, and epidemiologic characteristics (5). Several vasculitides can involve pulmonary vessels and lung parenchyma as primary or secondary targets. Not only the relative prevalence of vasculitides involving predominantly the pulmonary vessels is low (1–30 cases/100,000 inhabitants in the U.S.), but also their clinical presentation is usually diagnostically challenging (6,7). Radiologists play an important role in the management of pulmonary vasculitides, since they can provide supportive evidence for the diagnosis and opportunities for minimally invasive therapy.

This paper aims to present a practical approach for understanding the vasculitides that can affect the pulmonary vessels and lungs, using the revised Chapel Hill Consensus Conference Classification as reference. We will describe and illustrate the main radiologic findings, discussing opportunities for minimally invasive treatment. Presented cases were obtained from anonymized teaching files of the author's institutions. Informed consent was not obtained for this review paper.

Large vessel vasculitis

This group of vasculitides is characterized by chronic inflammation affecting elastic arteries (5). Takayasu (TAK) and giant cell arteritis (GCA) are the two diseases included in this group, and although both share common histopathologic features, they are epidemiologically distinct. Specifically, GCA usually affects individuals over

© Cardiovascular Diagnosis and Therapy. All rights reserved.

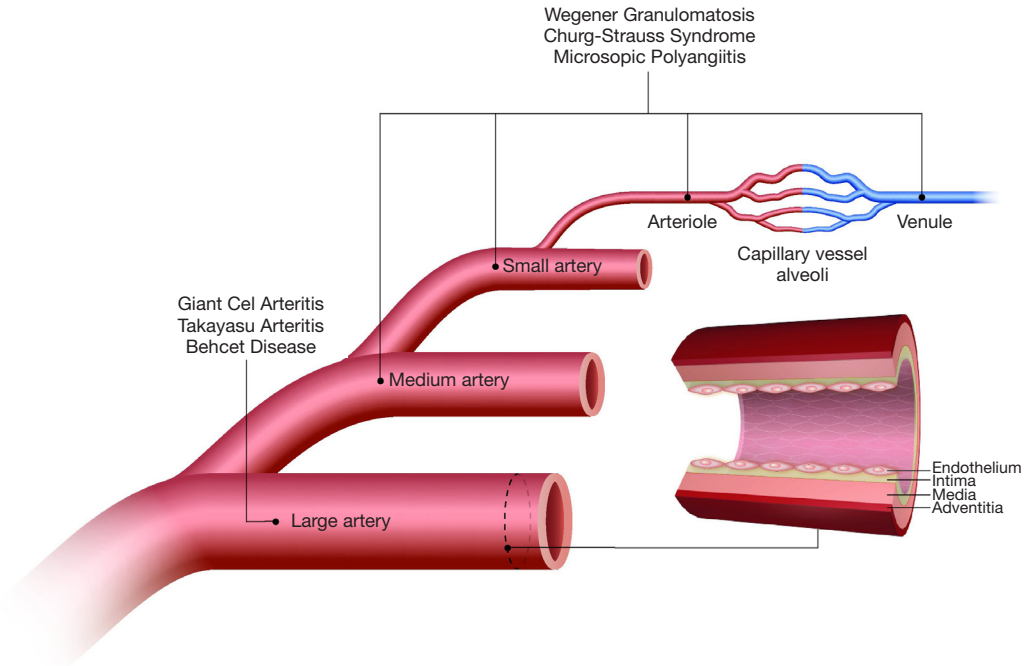

Figure 1 Scheme summarizing the Chapel Hill Vasculitides Classification, which groups systemic vasculitides according to caliber of the mainly involved vessels (Modified from Castañer E, Alguersuari A, Gallardo X, *et al*. When to suspect pulmonary vasculitis: radiologic and clinical clues. *Radiographics* 2010;30:33-53).

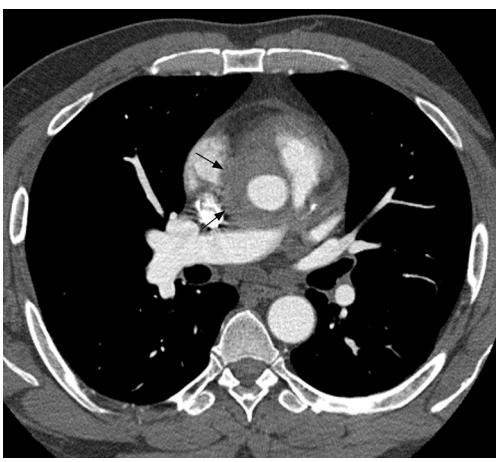

Figure 2 A 65-year-old male with large vessel vasculitis. Chest CT angiography showing circumferential arterial wall thickening in the ascending aorta (arrows). Biopsy later confirmed giant cell arteritis. Pulmonary involvement is rarely present in giant cell arteritis.

50 years, whereas TAK mainly occurs in adults younger than 40 years. Involvement of the pulmonary arteries in GCA is seldom present (8,9), and will not be discussed (*Figure 2*).

TAK arteritis

TAK is more commonly diagnosed in Asian countries, with estimated incidence of 1–2 cases per million per year in Japan, and prevalence of 40 cases per million. By contrast, the estimated prevalence of TAK in the U.S. is only 0.9 per million (7). The disease mainly affects women in their second and third decades of life (10,11). Although the disease etiology is still obscure, genetic links with HLA-B52, B39.2, and HLA-DR B1-1301/1302 have been described (10,12).

The natural history of TAK is divided into two phases, consisting of an inflammatory pre-pulseless stage, which is characterized by nonspecific inflammatory signs (e.g., fever, malaise, arthralgia, weight loss), followed by presentation with peripheral vascular insufficiency or dyspnea and chest pain related to vascular stenosis. A wide interval between the onset of symptoms and diagnosis is usually noted (11,13), and the clinical diagnostic criteria proposed for TAK can be found elsewhere (14). Histologically, TAK shares many features with GCA, including infiltration of T-cell lymphocytes and macrophages, characteristic of chronic granulomatous inflammation (15). One of the hallmarks is the presence of laminar media necrosis that is seen in two thirds

© Cardiovascular Diagnosis and Therapy. All rights reserved.

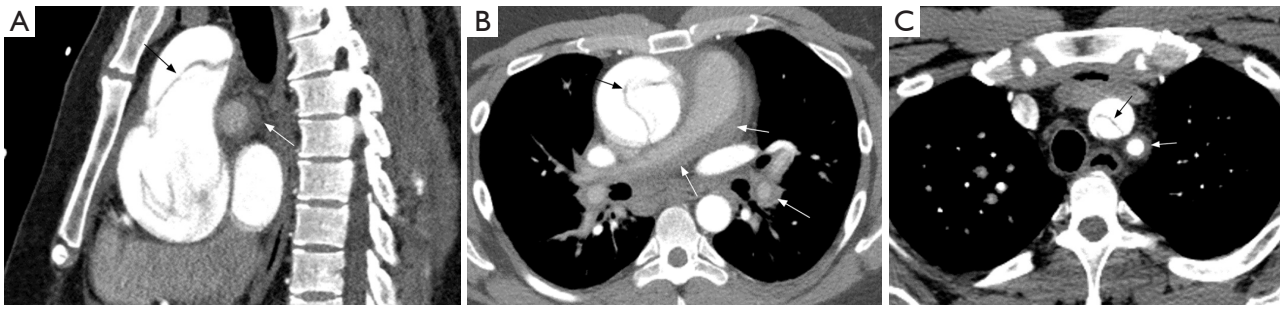

Figure 3 A 37-year-old Asian male presented with chest pain and was found to be hypertensive, with differential blood pressures between both arms. A CT with contrast demonstrated type A aortic dissection involving the ascending aorta (black arrows in A and B) and great vessels (black arrow in C). Also noted was extensive smooth concentric thickening of the pulmonary artery (white arrows in A and B), and subclavian artery (white arrow in C) without calcifications. Findings are likely secondary to underlying large vessel vasculitis such as type IV Takayasu or giant cell arteritis. Aortic dissection is a rare complication of Takayasu arteritis. Descending aorta is a more common location for dissection.

of the cases, consisting of interim mural infarction followed by loss of smooth muscle cells and collapse of the elastic fibers (15). Some features are unique to TAK, such as neutrophilic infiltrates and necrotizing inflammatory pattern, formation of micro abscesses, prominent adventitial thickening due to fibrosis, greater number of multinucleated giant cells, and conspicuous well-formed granulomas (15). The histologic features of pulmonary artery involvement are analogous to those found in aortitis. Elements specific to pulmonary artery involvement include stenosis and recanalization through collateral bronchial arteries (16).

Although pulmonary symptoms may be the first presentation in TAK (17), the definite frequency of pulmonary artery involvement is unknown, and reported values vary significantly depending on the sample and method of assessment. Studies without systematic evaluation of the pulmonary arteries found a relative low prevalence of TAK in this territory, varying from 7% (18) to 15% (19,20). Studies using systematic evaluation of the pulmonary circulation with magnetic resonance imaging (MRI) (21) and conventional angiography (22) found higher prevalence of 43% and 50%, respectively. Suzuki *et al.* studied 15 patients with TAK diagnosed by clinical criteria and arteriography with nuclear medicine perfusion scintigraphy, finding abnormal lung perfusion in 12 patients (80%), where only 17% (2/12) had presented with respiratory symptoms. Therefore, the true prevalence of pulmonary involvement in TAK is possibly underestimated (23).

Chest radiograph

Abnormal chest radiographs are found in 61% (65/107) to 67% (33/49) of TAK cases. Radiographic findings are, in decreasing order of frequency: irregular descending aortic contour, calcified aortic wall, dilated aortic arch, cardiomegaly, decreased pulmonary vascular markings, pulmonary arterial hypertension, pulmonary edema, calcified left subclavian artery, and rib notching (11,24).

Computed tomography angiography (CTA)

Although conventional angiography has been historically considered as the standard of reference for TAK diagnosis, multidetector CTA emerged as a reliable and non-invasive tool for depicting both luminal and mural lesions in the aorta and pulmonary artery (25), facilitating early phase disease detection (i.e., non-stenotic phase) and inflammatory activity monitoring (26). Park *et al.* evaluated the tomographic findings in 12 patients with TAK, finding variable vessel wall thickening (measuring ≥1 mm) and mural enhancement of the pulmonary artery trunk and main branches in two patients. They failed to demonstrate calcifications in the pulmonary arteries, a feature encountered in the thoracic aorta (19). These findings were confirmed in another study using multidetector CT scanners, with prevalence of mural thickening (range, 1–6 mm) in 2/15 TAK cases, with stenosis noted in 1/15 (27). *Figure 3* illustrates the application of CTA in TAK.

Magnetic resonance imaging

Computed tomography (CT) has been successfully used to study both lumen and vessel wall in TAK, but precise measurements of vessel wall thickness and enhancement are potentially impaired by highly attenuating intravascular contrast material. In addition, CTA requires the use of

© Cardiovascular Diagnosis and Therapy. All rights reserved.

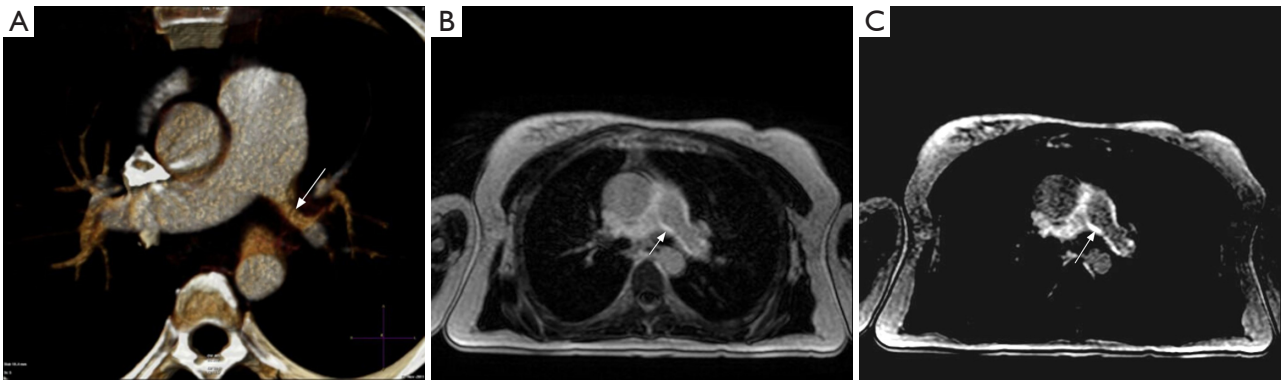

Figure 4 Young female with shortness of breath. Volume-rendered axial slab of pulmonary CT angiography showing severe stenosis of a long segment of the left pulmonary artery caused by Takayasu arteritis (arrow in A). Post-contrast T1-weighted gradient recalled-echo (GRE) (B) reveals diffuse enhancement in the pulmonary artery walls (arrow), which is confirmed on delayed post-contrast T1-weighted inversion-recovery ECG-gated GRE (C, arrow).

potentially nephrotoxic contrast material and exposure to ionizing radiation, which limit its applicability in repeat studies for disease monitoring. MRI has emerged as an alternative method without ionizing radiation, capable of combining vessel wall imaging with 3D magnetic resonance angiography and lung perfusion in a single study (21).

Yamada *et al.* studied 77 patients with spin-echo and cine gradient-echo techniques in a 1.5T MR scanner. A total of 70% (54/77) patients had abnormalities on MR images. Dilation of the pulmonary trunk was evident in 19% (15/77), treelike appearance of the peripheral pulmonary branches in 66% (51/77), and nodular thrombi in 3% (2/77). Accuracy was 90% (18/20) compared to conventional angiography and 88% (50/57) compared to perfusion scintigraphy (28). Matsunaga *et al.* studied 20 patients with TAK in a 1.5T MR scanner also using spin-echo and cine gradient-echo, comparing the MRI with CTA findings. In acute phase, the authors found thickening of the aortic and pulmonary artery walls, whereas in late occlusive phase, findings included stenosis, dilation, aneurysms, wall thickening, and mural thrombus. They also showed that presence of pulmonary artery involvement provided specificity to the diagnosis of TAK when aortic disease was present (29). Yamada *et al.* used a 3D breath-hold contrast-enhanced MRA sequence to study 30 cases of suspected TAK, 20 of them with confirmed disease. Pulmonary lesions were present on conventional angiography in 50% (10/20) of the patients, and MRA revealed all lesions with 100% sensitivity and specificity. Findings related to pulmonary artery involvement included poor visualization of peripheral pulmonary branches and areas of low signal intensity in the lung parenchyma reflecting hypoperfusion (30).

Non-contrast and contrast-enhanced techniques of vessel wall imaging have been used not only for detection of disease extent, but also to predict activity. Vessel wall enhancement on T1-weighted spin-echo imaging greater than myocardial enhancement has been associated with clinical and laboratorial signs of disease activity (31). The use of delayed enhancement images (i.e., acquired after 15 minutes of contrast injection) with ECG-gated inversion recovery prepared fast gradient-echo pulse sequences have also shown the potential to sensitize the evaluation of TAK, increasing the conspicuity of vessel wall thickening and enhancement by nulling the blood pool signal and adjacent mediastinal fat (32) (*Figure 4*). In addition, double-inversion spin-echo techniques ("black-blood imaging") have recently replaced conventional spin-echo sequences. A study combining black-blood imaging with post-contrast whole-body 3D MRA revealed vessel wall thickness ranging from 4 to 8.1 mm in active TAK *vs.* 2.7 to 5.6 mm in remissive patients. In 45% (19/42 patients), MRA revealed stenosis, occlusion, dilation, or aneurysm, with hypoperfusion in the lung parenchyma (21).

Shortcomings of MRA in comparison to other methods include longer scanning time and potential late complications, such as nephrogenic systemic fibrosis (NSF) and gadolinium deposition in the basal ganglia (33,34). Currently, use of gadolinium-based contrast agents is limited in patients with depressed renal function (i.e., estimated glomerular filtration rate <30 mL/min/1.73 m^2),

© Cardiovascular Diagnosis and Therapy. All rights reserved.

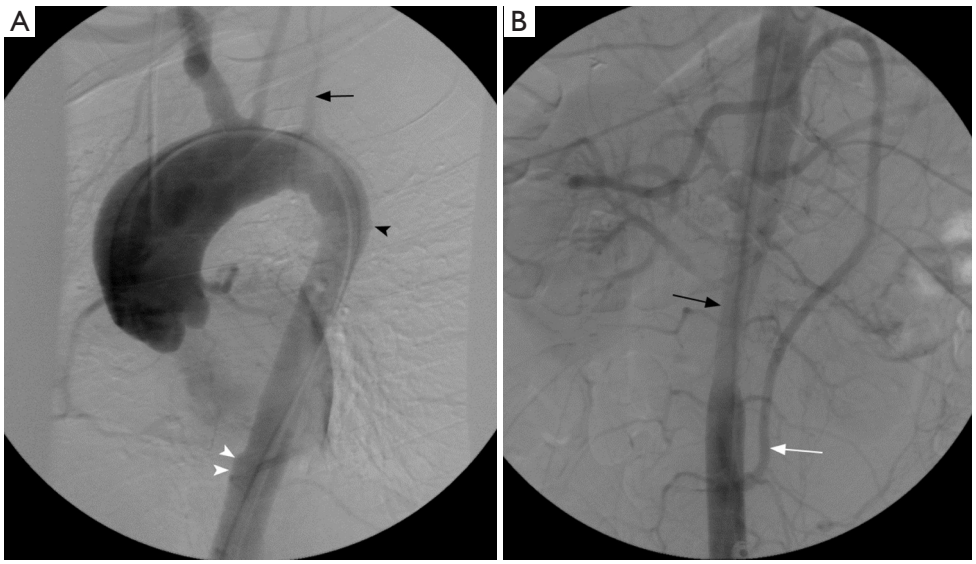

Figure 5 Aortogram images from a 25-year-old female with history of Takayasu arteritis demonstrates stenosis of the left proximal subclavian artery (black arrow in A), proximal descending thoracic aortic irregularity (black arrowhead in A), stenosis/occlusion of celiac artery and superior mesenteric artery (white arrowheads in A), and narrowing of the infra renal abdominal aorta (black arrow in B). The inferior mesenteric artery is hypertrophied and provides collaterals to superior mesenteric artery (white arrow in B).

especially group I agents (gadodiamide, gadopentetate dimeglumine, and gadoversetamide) (35). To this date, there is no definite evidence that gadolinium deposition in the basal ganglia is associated with harmful effects (36).

Conventional angiography

Lupi-Herrera *et al.* classified the disease according to 4 angiography patterns: type I, involvement of the aortic arch and supra-aortic trunks; type II, involvement of the descending thoracic aorta and abdominal aorta/branches; type III, involvement of the aortic arch, supra-aortic trunks, and abdominal aorta (*Figure 5*); type IV, involvement of the pulmonary arteries in addition to any other patterns. In their original paper, a retrospective analysis of conventional angiographic studies in 107 patients revealed type IV pattern in 16 cases of 35 undergoing pulmonary angiography (46%). Findings suggestive of TAK on conventional angiography included irregular internal surface of the vessel wall, stenosis, post-stenotic dilation, occlusion, and saccular aneurysm (11). Yamato *et al.* studied 21 patients with conventional pulmonary angiography, finding 18 abnormal studies (86%). The most common findings were occlusion or stenosis of main or lobar pulmonary artery branches with one case of main pulmonary artery dilation (24). There was no correlation between the extent of pulmonary arterial lesions and extent of systemic arteritis. Yamada *et al.* studied 98 patients with TAK, 30 of which had pulmonary arteriography in addition to aortic angiography. Pulmonary artery involvement was noted in 70% of the patients (21/30), with upper lobe pulmonary arterial branches being the most frequently affected. Collateral systemic artery-pulmonary artery communication was seen in 6% of all TAK patients (6/98) (37). Different series have also revealed systemic-pulmonary arterial shunts in TAK (38), including uncommon coronary-to-pulmonary artery shunts via bronchial arteries (39).

Endovascular therapy

Medical immunosuppressive therapy is usually implemented for induction of anti-inflammatory response and maintenance of remission, whereas bypass surgery has been proposed as the standard therapy for treating severe ischemic symptoms due to vascular occlusion or stenosis (40). Endovascular treatment may be considered as an alternative therapy modality with high rate of restenosis, especially during active inflammatory phase (41). Balloon angioplasty has been successfully used in the treatment of pulmonary artery stenosis in TAK (42,43). Restenosis has been described as a potential late complication of the procedure, even after stent deployment (42). Drug-eluting stents can

© Cardiovascular Diagnosis and Therapy. All rights reserved.

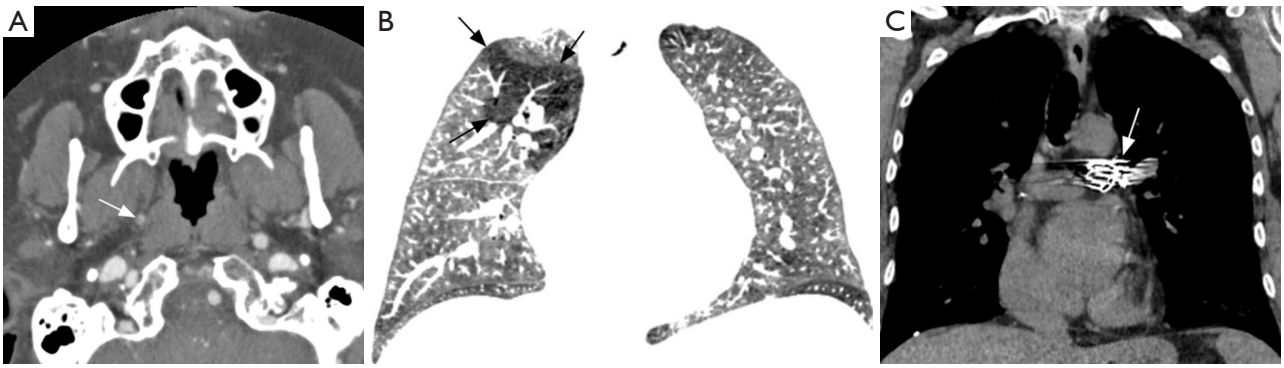

Figure 6 Takayasu arteritis affecting the pulmonary arteries and right internal carotid artery, endovascular treatment. Note the narrowing and wall thickening of the right common carotid artery (A, arrow) in this young patient. Mosaic attenuation with a large area of hypoperfusion on the minimum intensity projection (black arrows in B) coronal image of the caused by pulmonary vasculitis. A stent was placed in the left pulmonary artery to treat pulmonary stenosis (arrow in C).

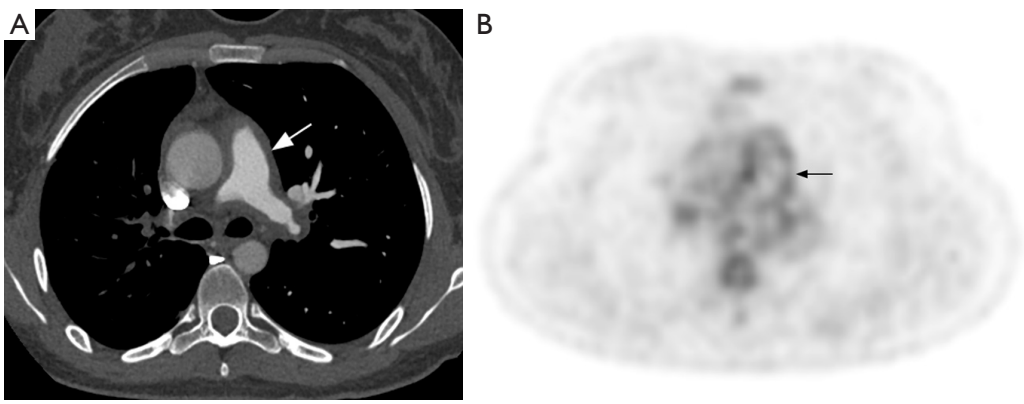

Figure 7 A 19-year-old female with shortness of breath and questioned chronic pulmonary embolism. Pulmonary CT angiography shows diffuse arterial wall thickening in the main pulmonary artery (arrow in A). 18F-FDG-PET shows matching diffuse low level radiotracer uptake in the pulmonary artery walls, not expected in chronic pulmonary embolism (arrow in B). The radiotracer uptake is consistent with active inflammatory process seen in Takayasu arteritis. Pulmonary sarcomas would present with higher 18F-FDG uptake in asymmetric masses occupying the arterial lumen and invading adjacent mediastinal structures.

modulate local inflammation, potentially reducing restenosis rates (44). Endovascular therapy should be postponed until resolution of active inflammation, with close maintenance of post intervention immunosuppressive treatment, for decreasing the risk or restenosis (45). *Figure 6* shows an example of endovascular treatment for left pulmonary artery stenosis in TAK.

Differential diagnosis

Major differential diagnoses of TAK include chronic pulmonary embolism (CPE) (46) and pulmonary artery sarcoma (47). Presence of concomitant aortitis is usually the main clue to the diagnosis of TAK. Although use of FDG-PET is extremely restricted in the evaluation of pulmonary hypertension, it may be used for distinguishing TAK and pulmonary sarcoma from CPE, as the first two diseases are generally FDG-avid, unlike CPE (48-50) (*Figure 7*).

Medium vessel vasculitis

Polyarteritis nodosa (PAN) and Kawasaki disease (KD) are non-ANCA associated necrotizing vasculitis mainly affecting medium sized arteries (5), and rarely affect the pulmonary arteries or lung parenchyma (51). Notwithstanding, an

© Cardiovascular Diagnosis and Therapy. All rights reserved.

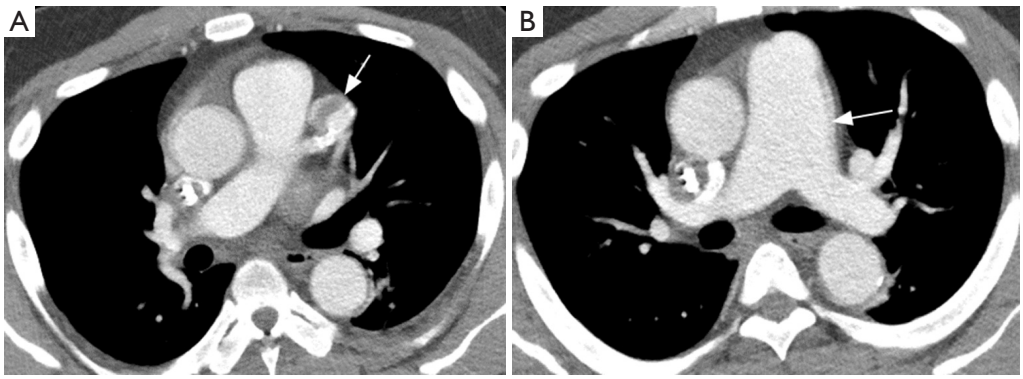

Figure 8 A 36-year-old male with past medical history of Kawasaki disease. Contrast-enhanced chest CT showing a partially thrombosed aneurysm of the left anterior descending coronary artery (arrow in A) and dilation of the main pulmonary artery, suggestive of pulmonary hypertension (arrow in B).

autopsy series of PAN cases showed involvement of the bronchial arteries in 70% of the patients (7/10) (52). The same study also found diffuse alveolar damage and lung fibrosis as possible lung parenchyma complications of PAN.

KD is one of the acute pediatric mucocutaneous lymph node syndromes, primarily affecting the coronary arteries, with occasional involvement of aorta and large arteries (5) (*Figure 8*). Although pulmonary artery involvement and symptomatic pulmonary manifestations of KD are infrequent, abnormal chest radiographs may be seen in up to 15% of the patients (53). Pulmonary nodules are the main presentation in chest radiographs, which correspond to mononuclear infiltrates on histopathologic specimens. The nodules are thought to reflect the host's response to an inhaled etiologic pathogen trigger in KD (54).

Small vessel vasculitis

The small pulmonary vessel vasculitides (i.e., affecting vessels less than 1 mm in diameter) are subdivided in two groups based on the presence or absence of anti-neutrophil cytoplasmic antibodies (ANCA), that are directed against intracellular antigens of neutrophils and monocytes. ANCA-associated vasculitides (AAV) comprise microscopic polyangiitis (MPA), granulomatosis with polyangiitis (GPA, formerly known as Wegner's granulomatosis), and eosinophilic granulomatosis with polyangiitis (EGPA, formerly Churg-Strauss syndrome) (5). The second group of ANCA negative vasculitides is caused by immune complex-mediated inflammation, and includes anti-glomerular basement membrane (GBM) disease (formerly Goodpasture syndrome), cryoglobulinemic vasculitis (CV), IgA vasculitis (formerly Henöch-Schonlein purpura), and hypocomplementemic urticarial vasculitis.

ANCA-associated vasculitides (AAV)

MPA, GPA, and EGPA are closely related forms of small vessel vasculitis. The inflammatory process affects mainly the arterioles, capillaries and venules, although involvement of medium and large-sized vessels is also seen (5,55). The annual incidence of AAV is about 20 per million (56,57). ANCA positivity can be distinguished into two main categories according to indirect immunofluorescence microscopy: cytoplasmic (C-ANCA) and perinuclear (P-ANCA). Diagnosis is obtained by clinical and serological evidence, requiring biopsy of the involved tissues in selected cases. In patients with suspected vasculitis, the identification of ANCA with specificity for myeloperoxidase (MPO) or proteinase 3 (PR3) indicates AAV with high probability. C-ANCA is primarily associated with antibodies directed against proteinase 3 located in azurophilic granules of neutrophils and monocytes. Nevertheless, patients with AAV can also be ANCA negative, and it remains uncertain whether ANCA-negativity is due to lack of sensitivity of available methods or presence of undiscovered ANCA types (5).

GPA and EGPA appear as necrotizing granulomatous inflammation on histopathology, whereas MPA presents with necrotizing inflammation without granulomatosis. Nodules, cavities or focal infiltrates related to GPA show a combination of vasculitis, geographic necrosis, and granulomatous inflammation (58). When diffuse alveolar hemorrhage (DAH) is present, pulmonary capillaritis is the usual finding, with infiltration of the neutrophils into the interstitial space

© Cardiovascular Diagnosis and Therapy. All rights reserved.

Figure 9 A 45-year-old male with ANCA-positive vasculitis, diagnosed as microscopic polyangiitis. Pretreatment axial CT image (A) showing patchy ground glass opacities (arrows) and peribronchial thickening, which resolved on the post treatment follow-up (B). Renal atrophy and nonspecific perinephric stranding was also note in the upper abdominal images (arrows in C).

and pulmonary capillaries wall. The release of toxic oxygen species enzymes from neutrophils causes fibrinoid necrosis of alveolar septae, thereby allowing erythrocytes to spill into the airspaces. EGPA patients may demonstrate simple eosinophilic pneumonia, or necrotizing vasculitis and granulomatous inflammation along with infiltration by eosinophils (59). Renal biopsies in patients with these disorders rarely reveal vasculitis, but rather demonstrate focal, segmental, necrotizing and crescentic glomerulonephritis (60) and can be distinguished from lupus or anti-GBM disease by the lack of significant immune deposits within the glomerulus (pauci-immune glomerulonephritis).

Microscopic polyangiitis (MPA)

MPA is the most frequent cause of pulmonary renal syndrome and is characterized by pulmonary capillaritis and glomerulonephritis. MPA is a non-granulomatous necrotizing small vessel vasculitis with involvement of the lungs, in about one-third of patients (61). It is regarded as the small-vessel variant of PAN. Almost all patients with MPA develop renal disease which is evident at the time of first presentation and is generally preceded by constitutional and musculoskeletal system symptoms (62-65). Palpable purpura is a common skin manifestation (66) and mesenteric vasculitis is twice as common in MPA compared to GPA, with about 30% of subjects being affected (67). There is no age predilection for microscopic polyangiitis (68).

Dyspnea, haemoptysis and progressive anaemia are common pulmonary symptoms. Clinically, pulmonary and renal manifestations are characteristic of anti-GBM syndrome, GPA and systemic lupus erythematosus (SLE). Differentiation is possible by testing for presence of anti-glomerular basement membrane antibodies, which are negative in MPA, GPA, and SLE. Renal biopsy can be used to differentiate MPA (non-granulomatous necrotizing systemic vasculitis) from GPA (granulomatous necrotizing vasculitis) and SLE (immune complex deposition vasculitis). Histopathology of biopsy specimens shows focal segmental necrotizing vasculitis and mixed inflammatory infiltrates and no evidence of granuloma formation, although this finding may be missed because of sampling errors (65). Fifty to seventy-five percent of patients with MPA are positive for P-ANCA and 35% to 65% are positive for anti-MPO. In a small group of patients, about 10% to 15%, the C-ANCA is positive (67,69).

Radiologically, MPA manifests as DAH secondary to pulmonary capillaritis (70). On chest radiography, this is seen as diffuse airspace opacities. CT is more informative in assessment of distribution of lung disease, showing patchy or diffuse bilateral ground glass opacities and consolidation (*Figure 9*). Typically, DAH involves the perihilar regions, sparing the lung apices and the costophrenic regions. The clinical evolution of DAH if not treated in a timely fashion can be fatal. The opacities may resolve in 1–2 weeks, unlike pulmonary edema which shows rapid change in evolution. Rarely, patients with chronic or recurrent alveolar hemorrhage may develop pulmonary fibrosis or chronic obstructive lung disease due to necrosis of binding alveolar walls. This finding is more common with MPA than with GPA (71-74). There is no distinct association between extent of fibrosis and DAH.

Granulomatosis with polyangiitis (GPA)

GPA affects adults between 30 and 60 years of age with equal prevalence in males and females but has been reported in all age groups (68). The main organs affected

© Cardiovascular Diagnosis and Therapy. All rights reserved.

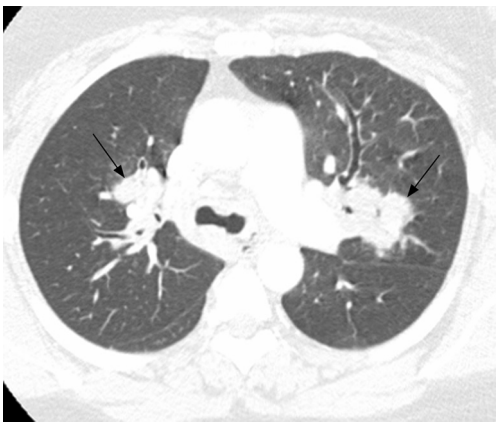

Figure 10 Middle-aged female, granulomatosis with polyangiitis. Axial chest CT image shows bilateral lobulated peribronchovascular masses and nodules (arrows), a rare manifestation of the disease.

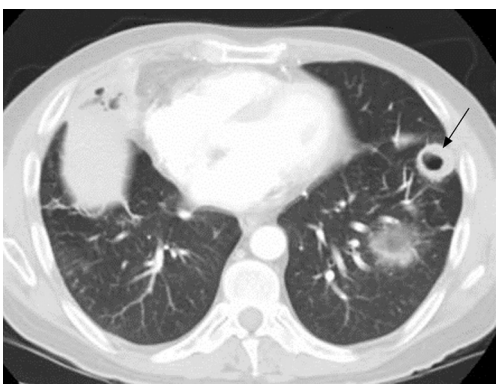

Figure 11 Chest CT of a young male showing thick-walled cavitary lesion in the left lower lobe (arrow), a common manifestation of granulomatosis with polyangiitis

by this small vessel vasculitides are renal, upper respiratory tract and lower respiratory tract. Pulmonary involvement is identified in 65% to 85% of patients with GPA. Upper airway disease develops in 90% of GPA patients, and manifests as chronic rhinosinusitis or epistaxis. Chest pain, dyspnea, hemoptysis are some of the lower respiratory tract manifestations. Eye involvement is reported in up to 25% with manifestations ranging from scleritis or optic neuritis to retroorbital pseudotumors. A minority of GPA patients have renal involvement at the time of presentation; however, it ultimately develops in 80% to 90%, manifesting as glomerulonephritis with symptoms of hematuria and azotemia (75). Central or peripheral nervous system and gastrointestinal tract can also be involved (62,76). An association with immunological diseases such as calcinosis, Raynaud phenomenon, esophageal dysmotility, sclerodactyly and telangiectasia (CREST) syndrome and Hashimoto's thyroiditis is described (77). Physical exam may reveal destructive changes in the nose such as septal perforation and saddle nose deformity. In addition, neutrophilic capillaritis, necrotizing vasculitis, bronchocentric eosinophilic capillaritis, and organizing pneumonia-like patterns have also been described (78). The presence of C-ANCA is seen in 90% to 95% of patients with active disease, but only in 63% of patients with inactive disease (79,80).

Pulmonary imaging manifestations on radiograph and CT range from single or multiple nodules, cavitary and non-cavitary masses, and focal or diffuse airspace disease (81). On CT, the nodules are seen to show a random distribution, with a slight predilection for subpleural region and are often related to vessels. Masses may also appear peribronchial or peribronchovascular and show irregular margins (81) (*Figure 10*). Their sizes vary from few millimeters to more than 10 centimeters, without a zonal predilection (82). The cavitation in the masses is generally thick walled with irregular and shaggy margins, although thin-walled cavities may also be seen (83) (*Figure 11*). Secondary infection of these cavities is not uncommon, and can be manifested as a new air-fluid level. Rim of ground glass opacity surrounding the lung nodules is present in about 15% cases representative of alveolar hemorrhage (78). Reverse halo appearance may also be seen (84). While lung nodules and consolidations are more prevalent in active phase, parenchymal bands and interlobular septal thickening may be seen in both active and quiescent phase. Ill-defined centrilobular nodules and or branching opacities have also been described in about 10% patients, likely reflecting presence of small vessel vasculitis (81). DAH develops in 5% to 10% patients and manifests as ground glass opacity or consolidation with central distribution (85). Crazy-paving pattern may also be seen with recurrent hemorrhage (*Figure 12*). Bronchial wall inflammation manifested as wall thickening involving the large and small airways in about 30% to 70% cases (78). Subglottic stenosis occurs in 15% of GPA patients and ulcerative tracheobronchitis and bronchial stenosis are well described complications of this disease entity (85,86). Pleural effusion, pleural thickening and mediastinal adenopathy may also be present (57,83). Surgical open lung biopsy is the gold standard technique for obtaining

© Cardiovascular Diagnosis and Therapy. All rights reserved.

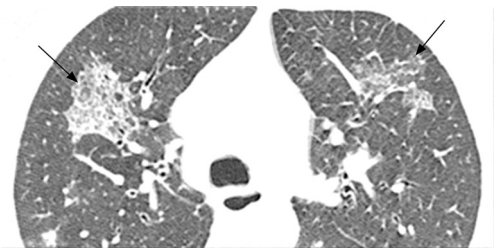

Figure 12 A 60-year-old female, granulomatosis with polyangiitis and symptoms of hemoptysis, aphthous ulcers, right eye conjunctivitis, hyperplastic lesions on vocal cords and rising creatinine. Combination of patchy geographic ground glass, some with septal thickening (crazy-paving appearance, arrows), presumably secondary to recurrent hemorrhage.

specimen as transbronchial biopsy (TBB) may not provide enough diagnostic tissue. Despite several attempts to define, diagnostic criteria for GPA, capable of differentiating it from microscopic polyangiitis, gaps in knowledge still exist (78). Diffuse lung disease with usual interstitial pneumonia (UIP) pattern has been reported in patients with AAV, although this finding is more common with MPA than with GPA (87). Advanced age of onset and early renal involvement, alveolar hemorrhage and anti-PR3 positivity are negative prognostic factors (88,89). GPA diagnosis remains a challenge in the light of imaging findings that can mimic other disease processes like infection. Patients with GPA are treated with immunosuppressive therapy, and CT is often performed to assess their response to treatment. In patients treated with immunosuppressive therapy, 50% of the nodules and masses resolve without scarring, and 40% diminish significantly with residual scar. Lesions involving the airways usually improve with treatment. Relapses with similar or different presentation may be seen and coexisting infection are common with GPA; in these cases, CT findings may be similar to or different from the initial presentation (57).

Eosinophilic granulomatosis with polyangiitis (EGPA)

EGPA consists of triad of tissue and blood eosinophilia, asthma, and small vessel vasculitis (90,91). The mean age of onset is in the third decade. Patients with EGPA often progress over a period of years from a prodromal phase with symptoms of respiratory involvement with chronic allergic rhinosinusitis, asthma and nasal polyposis, to the second phase in which peripheral blood eosinophilia and tissue eosinophilia predominate (92). If glucocorticoid therapy is not started at this point, further evolution to the vasculitic phase may occur (77). The lung is the most commonly involved organ, followed by the skin. Cardiac involvement occurs in about 40% of patients. Eosinophilic myocarditis, coronary arteritis, and pericardial effusion are some of the cardiac manifestations, and about 50% of the deaths occurred secondary to cardiac involvement (91,93,94). Peripheral neuropathy is noted in two thirds of EGPA patients during the course of their illness (95). Involvement of the kidneys is noted in only about 30% of patients. Histopathology findings include granulomatous necrotizing vasculitis of the small arteries and eosinophil-predominant inflammatory cells involving the bronchioles and peribronchial vessels. Activity in EGPA disease is characterized by positive P-ANCA or anti-MPO, and around 10% of patients show C-ANCA positivity (78). In the absence of ANCA positivity, tissue biopsy confirmation of an easily accessible tissue like skin is needed.

Radiographs most frequently show transient and migratory opacities, which are often bilateral and non-segmental in distribution. Patchy areas of ground glass opacities or consolidation with a peripheral predominance without zonal distribution are the most common imaging finding on HRCT. Pleural effusion may be identified in up to 30% (96) and may be secondary to eosinophilic pleuritis or cardiomyopathy (*Figure 13*). Interlobular septal thickening is best seen on CT, occurring in about 50% secondary to cardiogenic pulmonary edema, eosinophilic septal infiltration, or mild fibrosis (97). DAH is less common in this patient population, but airway involvement manifested as small peribronchial and centrilobular nodules, bronchial dilatation and bronchial wall thickening can be seen in about half the patients (91). Cavitation of the nodules is not a common feature (97).

Immune complex small vessel vasculitides

Anti-glomerular basement membrane disease

This entity is characterized by inflammation caused by autoantibody deposition in the capillary and glomerular basement membranes, which manifests as pulmonary hemorrhage and glomerulonephritis (5). The typical presentation of anti-GBM disease includes hemoptysis, dyspnea and iron deficiency anemia. On chest radiographs and CT, the classic presentation consists of bilateral and symmetric lung consolidation sparing the apices (98). CT may show patchy ground glass opacities before development of classic radiographic findings (*Figure 14*). The opacities

© Cardiovascular Diagnosis and Therapy. All rights reserved.

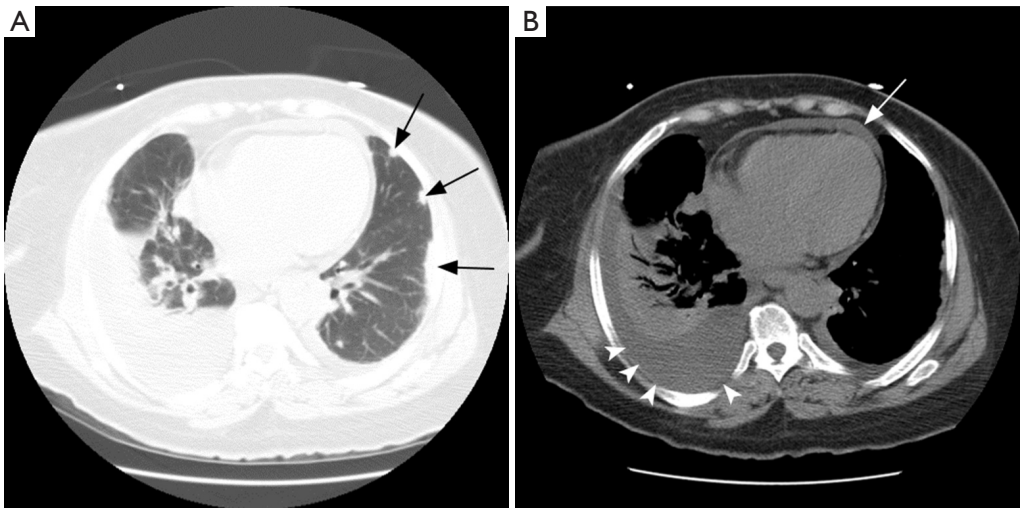

Figure 13 A 52-year-old male with eosinophilic polyangiitis. (A) Axial CT scan of the chest (lung windows) shows peripheral consolidations and opacities in the left lower lobe and lingula (arrows). (B) Note the pleural (arrowheads) and pericardial effusion (arrow) on the soft tissue window, secondary to pericardial involvement and myocarditis.

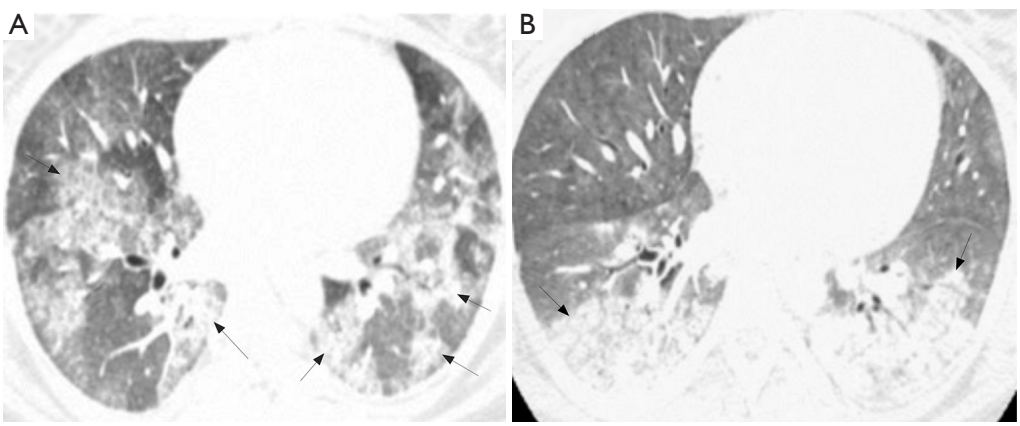

Figure 14 Young female with anti-GBM disease (Goodpasture's) and two CT studies more than 6 years apart showing recurrent bouts of diffuse alveolar hemorrhage (DAH). Axial CT images lung window centered at the level of the inferior pulmonary veins demonstrating shifting foci of consolidation and ground glass opacities (arrows in A and B).

tend to resolve within 2 to 3 days, replaced by linear opacities and thickened interlobular septa (98) (*Figure 15*). Pleural effusions are usually seen as result of either fluid overload or associated pneumonia. The diagnosis is established by detecting autoantibodies in the serum or by demonstration of linear antibody deposition along the glomerular basement membrane in renal biopsies (99). Lung biopsies are seldom necessary for diagnosis, but may show capillaritis and alveolar hemorrhage (100). Differential radiologic diagnosis includes other causes of alveolar hemorrhage.

Cryoglobulinemic vasculitis (CV)

This small-vessel vasculitis is caused by immune deposits involving serum cryoglobulins, affecting capillaries, venules, or arterioles in the skin, glomeruli, and peripheral nerves (5). Cryoglobulins are immunoglobulins that precipitate *in vitro* at temperatures below 37 ℃, causing damage by immune-mediated vasculitis or hyperviscosity. More than 90% of the cryoglobulinemia have a known underlying cause, such as

© Cardiovascular Diagnosis and Therapy. All rights reserved.

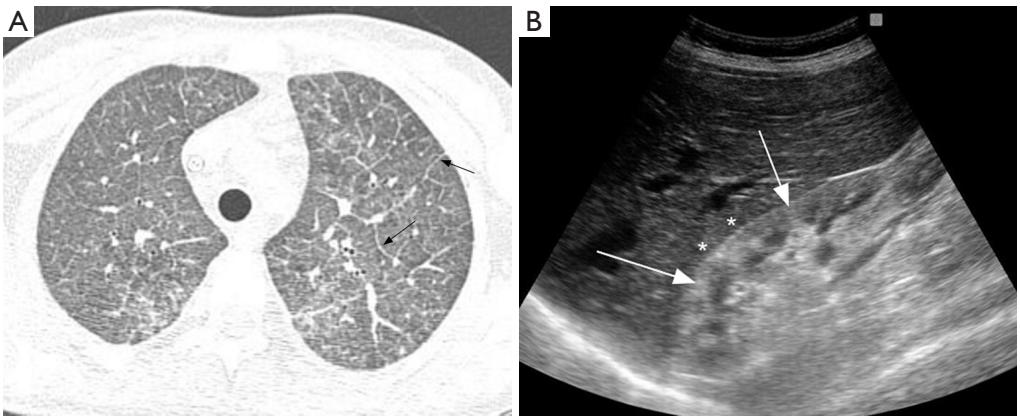

Figure 15 A 29-year-old female with anti-GBM disease presenting with alveolar hemorrhage and chronic kidney disease. Axial high-resolution CT image (A) shows diffuse underlying ground glass opacities with interlobular septal thickening consistent with resolving alveolar hemorrhage. Sagittal US image of the right flank (B) revealing increased echogenicity of the right kidney cortex (arrows) in comparison with the adjacent hepatic parenchyma (*), representing parenchymal renal disease.

infection (hepatitis C is the most common cause), autoimmune diseases, or cancer (101). Alveolar hemorrhage is the main pulmonary manifestation, especially in life-threatening cryoglobulinemic crises, usually associated with poor prognosis (102,103). Radiologically, the disease is indistinct from other causes of alveolar hemorrhage, and the diagnosis is established based on clinical and laboratorial findings.

IgA vasculitis (Henoch-Schönlein) (IgAV)

The immune deposits seen in this entity are predominantly composed of IgA1, resulting in inflammation of capillaries, venules, or arterioles in the skin, gastrointestinal tract, and joints (5). The clinical syndrome consists of palpable purpura without thrombocytopenia, abdominal pain, and arthritis, following an upper respiratory tract infection (104). Complications of IgAV include glomerulonephritis and gastrointestinal hemorrhage. Alveolar hemorrhage is a rare but fatal manifestation of IgAV (105-107).

Hypocomplementemic urticarial vasculitis (HUV) (anti-C1q vasculitis)

HUV is an uncommon type of vasculitis affecting capillaries, venules, or arterioles associated with the presence of serum anti-C1q antibodies and hypocomplementemia, clinically manifesting with urticaria, glomerulonephritis, arthritis, and ocular inflammation (5,108). Interestingly, HUV has been linked with obstructive pulmonary disease (109,110), and imaging studies may show basilar panacinar emphysema (111,112).

Variable vessel vasculitis

Behçet's disease (BD)

BD is a vasculitis affecting vessels of different calibers, originally occurring along the Silk Road and with current worldwide occurrence given to immigration (113). Worldwide prevalence may vary from as low as less than 1 case per 100,000 inhabitants to 370 cases per 10,000 inhabitants (113). A male predominance has been suggested, although there is heterogeneity of male-to-female ratio among different geographic areas (113). The clinical presentation includes recurrent mucocutaneous ulcers and iridocyclitis. There is currently no pathognomonic test for the diagnosis of BD, which still relies on a combination of mainly clinical criteria (114). Overall, vascular involvement has been described in 2% to 32% of the patients depending on the geographic region (113). Many different pulmonary manifestations have been reported, involving not only lung vessels, but also parenchyma, airways, and pleura (115).

On histopathology, BD involves large and small vessels and is characterized by lymphocytic and necrotizing vasculitis, leading to destruction of elastic and muscular fibers of arteries, leading to the formation aneurysms of elastic arteries, thrombosis, and infarcts (116). Pulmonary arteries are second to the aorta in frequency of vascular involvement, with aneurysms being more frequent than thrombosis (117). Pulmonary artery aneurysms (PAA) most frequently present

© Cardiovascular Diagnosis and Therapy. All rights reserved.

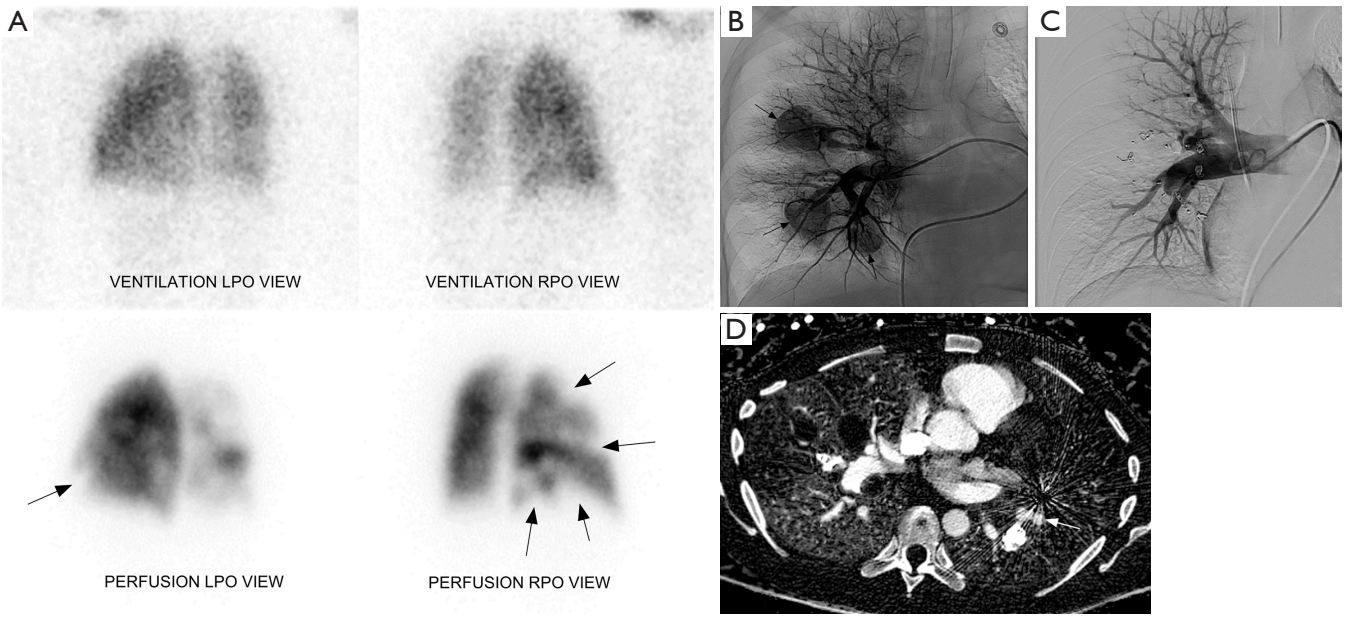

Figure 16 A 38-year-old male with history of Bechet's syndrome was noted to have pulmonary arterial aneurysms, dilatation and segmental filling defects on CT imaging (not shown here) on initial work up for pulmonary hypertension. A VQ scan (A) demonstrates multiple mismatched perfusion segmental defects (arrows) consistent with a high probability scan for pulmonary embolism. Subsequently, the patient presented with massive hemoptysis. A right pulmonary arteriogram demonstrates multiple pulmonary arterial aneurysms (arrows in B) which were successfully embolized with coils and plugs (C). On follow up, spectral CT images easily demonstrate residual opacification (arrow) of one of the left lower lobe aneurysm previously treated with an Amplatzer vascular pug (D).

with hemoptysis, carrying a high mortality rate of 50% in 10 months (118) (*Figure 16*). On chest radiographs, PAA most commonly manifests as lobular dilation of the descending branches of the pulmonary artery in both hila (119). Conventional angiography may confirm dilation of the pulmonary artery branches, also showing vessel occlusion (120), which occurs as frequently as in 50% of the cases (119). However, chest CT is commonly preferred to conventional angiography due to the risks of dissection and pseudoaneurysm formation with the latter (119). On chest CT, PAA usually measure from 1 to 7 cm, occurring in the main pulmonary arteries or lobar branches in up to 78% of the times (121). As with conventional angiography, thrombosis is commonly seen in 33% of the PAA at the initial diagnosis, and its prevalence increases during treatment (121). The most common parenchymal signs include perianeurysmal consolidation or air-space nodules and mosaic attenuation, which most commonly reflect hemorrhage or infarcts (121). Organizing pneumonia has also been described as cause of perianeurysmal air-space opacities in BD (122). Resolution of up to 76% of the PAA may occur with immunosuppressive therapy, with clearance of the perianeurysmal opacities in 1–5 months (121). MR angiography may also be used as a substitute for chest CT and conventional angiography for the assessment of PAA (123).

Endovascular treatment of aneurysms with stents and embolization of pulmonary artery bleeding are some of the situations where interventional radiology may act effectively (124,125) (*Figures 16,17*). However, depending on the size, number and location of the aneurysms, lack of adequate access (e.g., such as occlusion of the superior or inferior vena cava), endovascular therapy might not be feasible.

Analogous to BD, Hughes-Stovin syndrome is also an uncommon disease characterized by PAA and systemic thrombosis. Although some controversy exists, given the similarities, it is believed that they correspond to the same entity (126).

Vasculitis associated with systemic disease

Differentiation between primary and secondary causes is evolving as more etiologies for secondary vasculitis are discovered (5). Collagen vascular disease is a well-

© Cardiovascular Diagnosis and Therapy. All rights reserved.

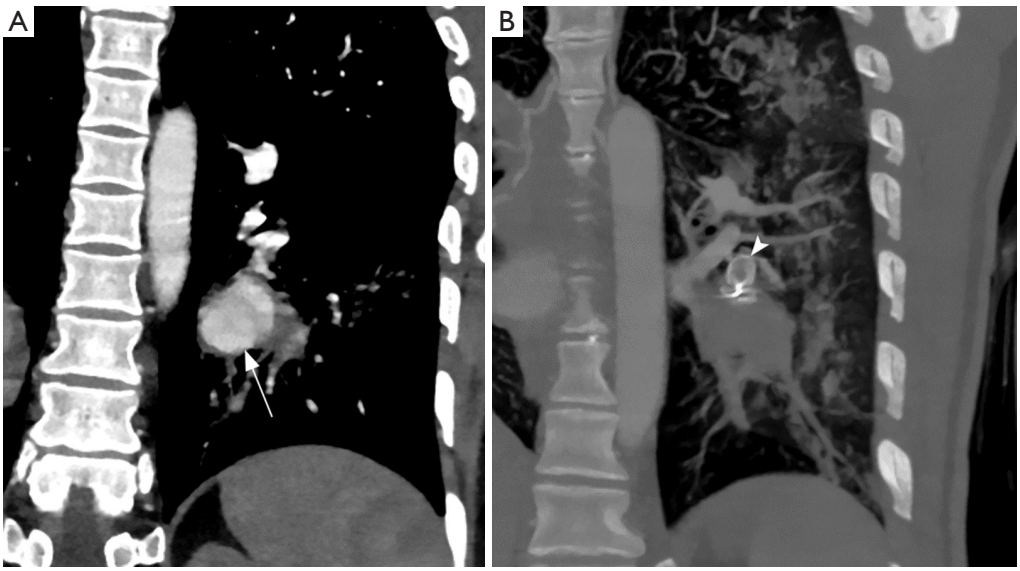

Figure 17 Coronal CT angiography showing pulmonary artery aneurysm (arrow) in a young male with Bechet's disease before (A) and after Amplatzer plug embolization (arrowhead in B). Embolization can be performed with vascular plug, coil or both.

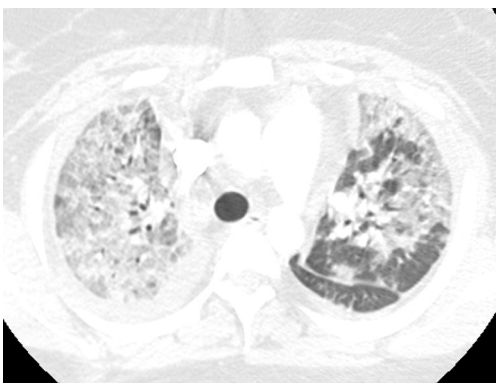

Figure 18 Diffuse pulmonary hemorrhage in a 33-year-old female with history of systemic lupus erythematosus who presented with shortness of breath. Axial CT image show diffuse ground glass opacities involving right greater than left lung. Possibilities of diffuse alveolar hemorrhage, lupus pneumonitis, infection and ARDS are entertained. A subsequent bronchoalveolar lavage revealed pulmonary hemorrhage.

recognized cause of pulmonary capillaritis and DAH (127,128). Capillaritis is the most common manifestation as the small vessels are most frequently involved in secondary vasculitis. Cavitary centrilobular nodules are an infrequent finding (129,130). SLE has the most frequently association with capillaritis and DAH (131,132) with approximately 3% incidence (133) (*Figure 18*). SLE patients may also occasionally exhibit pulmonary hypertension which is responsive to immunosuppression, suggesting an underlying inflammatory vascular process (134). Additional findings secondary to cavitary infarcts, congestive heart failure, aspiration, infection and lupus pneumonitis may also be seen. Rheumatoid arthritis (RA), systemic sclerosis, mixed connective tissue disease, sarcoidosis, relapsing polymyositis, and the related anti-synthetase antibody syndrome are other reported causes (135,136). RA-related pulmonary vasculitis may be confined to the lungs (isolated vasculitis) (135,136). Vasculitic skin ulcers and peripheral neuropathies are additional clues to the presence of rheumatoid vasculitis. Chest radiograph in these patients may be normal or may show signs of pulmonary hypertension and interstitial opacities. Focal and diffuse alveolar opacities and consolidations secondary to DAH can be seen (135).

Pulmonary vasculitis is an occasional complication of drug use, and infection. Propylthiouracil is the best-known drug associated with the development of ANCA-associated systemic vasculitis (137). Retinoic acid syndrome, crack cocaine and diphenylhydantoin can also cause capillaritis and DAH (137,138), while injected talc used as fillers in capsules may cause giant cell reaction around arterioles, which may manifest as centrilobular nodules (139). Certain bacterial organisms including *Legionella*, *Pseudomonas* and *Staphylococcus* species may cause inflammatory reaction and destruction of blood vessels in the lungs. The

© Cardiovascular Diagnosis and Therapy. All rights reserved.

angioinvasive fungi, Aspergillus and Mucor, may cause pulmonary infarction as a result of vascular occlusion, or massive bleeding due to rupture of mycotic pulmonary arterial aneurysms. *Dirofilaria immitis*, the dog tapeworm, and *Pneumocystis jiroveci* infection are some rare causes of pulmonary vasculitis (140,141).

Conclusions

Diagnosis of pulmonary vasculitis can be challenging given the myriad of clinical features and etiologies which may mimic infection, malignancy, and connective tissue disorder. Imaging patterns include, but are not limited to, localized or diffuse opacities, nodules, cavities, pulmonary artery enlargement and perfusion changes. Radiologists play an important role in pulmonary vasculitis management by providing supportive diagnostic evidence and minimally invasive therapeutic approaches.

Acknowledgements

None.

Footnote

Conflicts of Interest: The authors have no conflicts of interest to declare.

References

1. Weyand CM, Goronzy JJ. Immune mechanisms in medium and large-vessel vasculitis. Nat Rev Rheumatol 2013;9:731-40.
2. Travis WD. Pathology of pulmonary vasculitis. Semin Respir Crit Care Med 2004;25:475-82.
3. Lie JT. Diagnostic histopathology of major systemic and pulmonary vasculitic syndromes. Rheum Dis Clin North Am 1990;16:269-92.
4. Jennette JC, Falk RJ, Andrassy K, et al. Nomenclature of systemic vasculitides. Proposal of an international consensus conference. Arthritis Rheum 1994;37:187-92.
5. Jennette JC, Falk RJ, Bacon PA, et al. 2012 revised International Chapel Hill Consensus Conference Nomenclature of Vasculitides. Arthritis Rheum 2013;65:1-11.
6. Frankel SK, Schwarz MI. The pulmonary vasculitides. Am J Respir Crit Care Med 2012;186:216-24.
7. Onen F, Akkoc N. Epidemiology of Takayasu arteritis. Presse Med 2017;46:e197-203.
8. Brister SJ, Wilson-Yang K, Lobo FV, et al. Pulmonary thromboendarterectomy in a patient with giant cell arteritis. Ann Thorac Surg 2002;73:1977-9.
9. Doyle L, McWilliam L, Hasleton PS. Giant cell arteritis with pulmonary involvement. Br J Dis Chest 1988;82:88-92.
10. Kobayashi Y, Numano F. 3. Takayasu arteritis. Intern Med 2002;41:44-6.
11. Lupi-Herrera E, Sanchez-Torres G, Marcushamer J, et al. Takayasu's arteritis. Clinical study of 107 cases. Am Heart J 1977;93:94-103.
12. Arnaud L, Haroche J, Mathian A, et al. Pathogenesis of Takayasu's arteritis: a 2011 update. Autoimmun Rev 2011;11:61-7.
13. Johnston SL, Lock RJ, Gompels MM. Takayasu arteritis: a review. J Clin Pathol 2002;55:481-6.
14. Arend WP, Michel BA, Bloch DA, et al. The American College of Rheumatology 1990 criteria for the classification of Takayasu arteritis. Arthritis Rheum 1990;33:1129-34.
15. Miller DV, Maleszewski JJ. The pathology of large-vessel vasculitides. Clin Exp Rheumatol 2011;29:S92-8.
16. Matsubara O, Yoshimura N, Tamura A, et al. Pathological features of the pulmonary artery in Takayasu arteritis. Heart Vessels Suppl 1992;7:18-25.
17. Hayashi K, Nagasaki M, Matsunaga N, et al. Initial pulmonary artery involvement in Takayasu arteritis. Radiology 1986;159:401-3.
18. Bicakcigil M, Aksu K, Kamali S, et al. Takayasu's arteritis in Turkey - clinical and angiographic features of 248 patients. Clin Exp Rheumatol 2009;27:S59-64.
19. Park JH, Chung JW, Im JG, et al. Takayasu arteritis: evaluation of mural changes in the aorta and pulmonary artery with CT angiography. Radiology 1995;196:89-93.
20. Chae EJ, Do KH, Seo JB, et al. Radiologic and clinical findings of Behcet disease: comprehensive review of multisystemic involvement. Radiographics 2008;28:e31.
21. Li D, Lin J, Yan F. Detecting disease extent and activity of Takayasu arteritis using whole-body magnetic resonance angiography and vessel wall imaging as a 1-stop solution. J Comput Assist Tomogr 2011;35:468-74.
22. Lupi E, Sanchez G, Horwitz S, et al. Pulmonary artery involvement in Takayasu's arteritis. Chest 1975;67:69-74.
23. Suzuki Y, Konishi K, Hisada K. Radioisotope lung scanning in Takayasu's arteritis. Radiology 1973;109:133-6.
24. Yamato M, Lecky JW, Hiramatsu K, et al. Takayasu arteritis: radiographic and angiographic findings in 59 patients. Radiology 1986;161:329-34.

© Cardiovascular Diagnosis and Therapy. All rights reserved.

25. Park JH, Chung JW, Lee KW, et al. CT angiography of Takayasu arteritis: comparison with conventional angiography. J Vasc Interv Radiol 1997;8:393-400.
26. Paul JF, Fiessinger JN, Sapoval M, et al. Follow-up electron beam CT for the management of early phase Takayasu arteritis. J Comput Assist Tomogr 2001;25:924-31.
27. Khandelwal N, Kalra N, Garg MK, et al. Multidetector CT angiography in Takayasu arteritis. Eur J Radiol 2011;77:369-74.
28. Yamada I, Numano F, Suzuki S. Takayasu arteritis: evaluation with MR imaging. Radiology 1993;188:89-94.
29. Matsunaga N, Hayashi K, Sakamoto I, et al. Takayasu arteritis: MR manifestations and diagnosis of acute and chronic phase. J Magn Reson Imaging 1998;8:406-14.
30. Yamada I, Nakagawa T, Himeno Y, et al. Takayasu arteritis: diagnosis with breath-hold contrast-enhanced three-dimensional MR angiography. J Magn Reson Imaging 2000;11:481-7.
31. Choe YH, Han BK, Koh EM, et al. Takayasu's arteritis: assessment of disease activity with contrast-enhanced MR imaging. AJR Am J Roentgenol 2000;175:505-11.
32. Desai MY, Stone JH, Foo TK, et al. Delayed contrast-enhanced MRI of the aortic wall in Takayasu's arteritis: initial experience. AJR Am J Roentgenol 2005;184:1427-31.
33. Zhang B, Liang L, Chen W, et al. An Updated Study to Determine Association between Gadolinium-Based Contrast Agents and Nephrogenic Systemic Fibrosis. PLoS One 2015;10:e0129720.
34. Kanda T, Nakai Y, Hagiwara A, et al. Distribution and chemical forms of gadolinium in the brain: a review. Br J Radiol 2017;90:20170115.
35. ACR Committee on Drugs and Contrast Media. Manual on Contrast Media v10.3. 2017. Available online: https://www.acr.org/Quality-Safety/Resources/Contrast-Manual. Accessed 11/30/2017.
36. FDA. FDA Drug Safety Communication: FDA identifies no harmful effects to date with brain retention of gadolinium-based contrast agents for MRIs; review to continue. 2017. Available online: https://www.fda.gov/Drugs/DrugSafety/ucm559007.htm. Accessed 11/30/2017.
37. Yamada I, Shibuya H, Matsubara O, et al. Pulmonary artery disease in Takayasu's arteritis: angiographic findings. AJR Am J Roentgenol 1992;159:263-9.
38. Ishikawa T. Systemic artery--pulmonary artery communication in Takayasu's arteritis. AJR Am J Roentgenol 1977;128:389-93.
39. Matsunaga N, Hayashi K, Sakamoto I, et al. Coronary-to-pulmonary artery shunts via the bronchial artery: analysis of cineangiographic studies. Radiology 1993;186:877-82.
40. Isobe M. Takayasu arteritis revisited: current diagnosis and treatment. Int J Cardiol 2013;168:3-10.
41. Park JH, Han MC, Kim SH, et al. Takayasu arteritis: angiographic findings and results of angioplasty. AJR Am J Roentgenol 1989;153:1069-74.
42. Li D, Ma S, Li G, et al. Endovascular stent implantation for isolated pulmonary arterial stenosis caused by Takayasu's arteritis. Clin Res Cardiol 2010;99:573-5.
43. Qin L, Hong-Liang Z, Zhi-Hong L, et al. Percutaneous transluminal angioplasty and stenting for pulmonary stenosis due to Takayasu's arteritis: clinical outcome and four-year follow-up. Clin Cardiol 2009;32:639-43.
44. Jin SA, Lee JH, Park JH, et al. Endovascular treatment in a patient with left main coronary and pulmonary arterial stenoses as an initial manifestation of Takayasu's arteritis. Heart Lung Circ 2015;24:e26-30.
45. Park MC, Lee SW, Park YB, et al. Post-interventional immunosuppressive treatment and vascular restenosis in Takayasu's arteritis. Rheumatology (Oxford) 2006;45:600-5.
46. Auger WR, Fedullo PF, Moser KM, et al. Chronic major-vessel thromboembolic pulmonary artery obstruction: appearance at angiography. Radiology 1992;182:393-8.
47. Kauczor HU, Schwickert HC, Mayer E, et al. Pulmonary artery sarcoma mimicking chronic thromboembolic disease: computed tomography and magnetic resonance imaging findings. Cardiovasc Intervent Radiol 1994;17:185-9.
48. Webb M, Chambers A, AL-Nahhas A, et al. The role of 18F-FDG PET in characterising disease activity in Takayasu arteritis. Eur J Nucl Med Mol Imaging 2004;31:627-34.
49. Kobayashi Y, Ishii K, Oda K, et al. Aortic wall inflammation due to Takayasu arteritis imaged with 18F-FDG PET coregistered with enhanced CT. J Nucl Med 2005;46:917-22.
50. Meller J, Grabbe E, Becker W, et al. Value of F-18 FDG hybrid camera PET and MRI in early takayasu aortitis. Eur Radiol 2003;13:400-5.
51. Nick J, Tuder R, May R, et al. Polyarteritis nodosa with pulmonary vasculitis. Am J Respir Crit Care Med 1996;153:450-3.
52. Matsumoto T, Homma S, Okada M, et al. The lung in polyarteritis nodosa: a pathologic study of 10 cases. Hum Pathol 1993;24:717-24.
53. Umezawa T, Saji T, Matsuo N, et al. Chest x-ray findings in the acute phase of Kawasaki disease. Pediatr Radiol

© Cardiovascular Diagnosis and Therapy. All rights reserved.

1989;20:48-51.
54. Freeman AF, Crawford SE, Finn LS, et al. Inflammatory pulmonary nodules in Kawasaki disease. Pediatr Pulmonol 2003;36:102-6.
55. Falk RJ, Nachman PH, Hogan SL, et al. ANCA glomerulonephritis and vasculitis: a Chapel Hill perspective. Semin Nephrol 2000;20:233-43.
56. Watts RA, Lane SE, Bentham G, et al. Epidemiology of systemic vasculitis: a ten-year study in the United Kingdom. Arthritis Rheum 2000;43:414-9.
57. Lee KS, Kim TS, Fujimoto K, et al. Thoracic manifestation of Wegener's granulomatosis: CT findings in 30 patients. Eur Radiol 2003;13:43-51.
58. Travis WD, Hoffman GS, Leavitt RY, et al. Surgical pathology of the lung in Wegener's granulomatosis. Review of 87 open lung biopsies from 67 patients. Am J Surg Pathol 1991;15:315-33.
59. Travis WD. Pathology of pulmonary granulomatous vasculitis. Sarcoidosis Vasc Diffuse Lung Dis 1996;13:14-27.
60. Jennette JC, Falk RJ. The pathology of vasculitis involving the kidney. Am J Kidney Dis 1994;24:130-41.
61. Lhote F, Cohen P, Guillevin L. Polyarteritis nodosa, microscopic polyangiitis and Churg-Strauss syndrome. Lupus 1998;7:238-58.
62. Frankel SK, Cosgrove GP, Fischer A, et al. Update in the diagnosis and management of pulmonary vasculitis. Chest 2006;129:452-65.
63. Marten K, Schnyder P, Schirg E, et al. Pattern-based differential diagnosis in pulmonary vasculitis using volumetric CT. AJR Am J Roentgenol 2005;184:720-33.
64. Sorensen SF, Slot O, Tvede N, et al. A prospective study of vasculitis patients collected in a five year period: evaluation of the Chapel Hill nomenclature. Ann Rheum Dis 2000;59:478-82.
65. Guillevin L, Durand-Gasselin B, Cevallos R, et al. Microscopic polyangiitis: clinical and laboratory findings in eighty-five patients. Arthritis Rheum 1999;42:421-30.
66. Akikusa B, Sato T, Ogawa M, et al. Necrotizing alveolar capillaritis in autopsy cases of microscopic polyangiitis. Incidence, histopathogenesis, and relationship with systemic vasculitis. Arch Pathol Lab Med 1997;121:144-9.
67. Savage CO, Winearls CG, Evans DJ, et al. Microscopic polyarteritis: presentation, pathology and prognosis. Q J Med 1985;56:467-83.
68. Seo P, Stone JH. The antineutrophil cytoplasmic antibody-associated vasculitides. Am J Med 2004;117:39-50.
69. Bosch X, Guilabert A, Font J. Antineutrophil cytoplasmic antibodies. Lancet 2006;368:404-18.
70. Lauque D, Cadranel J, Lazor R, et al. Microscopic polyangiitis with alveolar hemorrhage. A study of 29 cases and review of the literature. Groupe d'Etudes et de Recherche sur les Maladies "Orphelines" Pulmonaires (GERM"O"P). Medicine (Baltimore) 2000;79:222-33.
71. Brugiere O, Raffy O, Sleiman C, et al. Progressive obstructive lung disease associated with microscopic polyangiitis. Am J Respir Crit Care Med 1997;155:739-42.
72. Nada AK, Torres VE, Ryu JH, et al. Pulmonary fibrosis as an unusual clinical manifestation of a pulmonary-renal vasculitis in elderly patients. Mayo Clin Proc 1990;65:847-56.
73. Homma S, Matsushita H, Nakata K. Pulmonary fibrosis in myeloperoxidase antineutrophil cytoplasmic antibody-associated vasculitides. Respirology 2004;9:190-6.
74. Jennette JC, Thomas DB, Falk RJ. Microscopic polyangiitis (microscopic polyarteritis). Semin Diagn Pathol 2001;18:3-13.
75. Fauci AS, Haynes BF, Katz P, et al. Wegener's granulomatosis: prospective clinical and therapeutic experience with 85 patients for 21 years. Ann Intern Med 1983;98:76-85.
76. Brown KK. Pulmonary vasculitis. Proc Am Thorac Soc 2006;3:48-57.
77. Feragalli B, Mantini C, Sperandeo M, et al. The lung in systemic vasculitis: radiological patterns and differential diagnosis. Br J Radiol 2016;89:20150992.
78. Mahmoud S, Ghosh S, Farver C, et al. Pulmonary Vasculitis: Spectrum of Imaging Appearances. Radiol Clin North Am 2016;54:1097-118.
79. Bligny D, Mahr A, Toumelin PL, et al. Predicting mortality in systemic Wegener's granulomatosis: a survival analysis based on 93 patients. Arthritis Rheum 2004;51:83-91.
80. Nolle B, Specks U, Ludemann J, et al. Anticytoplasmic autoantibodies: their immunodiagnostic value in Wegener granulomatosis. Ann Intern Med 1989;111:28-40.
81. Aberle DR, Gamsu G, Lynch D. Thoracic manifestations of Wegener granulomatosis: diagnosis and course. Radiology 1990;174:703-9.
82. Castaner E, Alguersuari A, Gallardo X, et al. When to suspect pulmonary vasculitis: radiologic and clinical clues. Radiographics 2010;30:33-53.
83. Komocsi A, Reuter M, Heller M, et al. Active disease and residual damage in treated Wegener's granulomatosis: an observational study using pulmonary high-resolution computed tomography. Eur Radiol 2003;13:36-42.
84. Ananthakrishnan L, Sharma N, Kanne JP. Wegener's

© Cardiovascular Diagnosis and Therapy. All rights reserved.

granulomatosis in the chest: high-resolution CT findings. AJR Am J Roentgenol 2009;192:676-82.
85. Comarmond C, Crestani B, Tazi A, et al. Pulmonary fibrosis in antineutrophil cytoplasmic antibodies (ANCA)-associated vasculitis: a series of 49 patients and review of the literature. Medicine (Baltimore) 2014;93:340-9.
86. Lohrmann C, Uhl M, Kotter E, et al. Pulmonary manifestations of wegener granulomatosis: CT findings in 57 patients and a review of the literature. Eur J Radiol 2005;53:471-7.
87. Attali P, Begum R, Ban Romdhane H, et al. Pulmonary Wegener's granulomatosis: changes at follow-up CT. Eur Radiol 1998;8:1009-113.
88. Neumann I, Kain R, Regele H, et al. Histological and clinical predictors of early and late renal outcome in ANCA-associated vasculitis. Nephrol Dial Transplant 2005;20:96-104.
89. Holle JU, Gross WL, Holl-Ulrich K, et al. Prospective long-term follow-up of patients with localised Wegener's granulomatosis: does it occur as persistent disease stage? Ann Rheum Dis 2010;69:1934-9.
90. Conron M, Beynon HL. Churg-Strauss syndrome. Thorax 2000;55:870-7.
91. Guillevin L, Cohen P, Gayraud M, et al. Churg-Strauss syndrome. Clinical study and long-term follow-up of 96 patients. Medicine (Baltimore) 1999;78:26-37.
92. Churg A. Recent advances in the diagnosis of Churg-Strauss syndrome. Mod Pathol 2001;14:1284-93.
93. Lanham JG, Elkon KB, Pusey CD, et al. Systemic vasculitis with asthma and eosinophilia: a clinical approach to the Churg-Strauss syndrome. Medicine (Baltimore) 1984;63:65-81.
94. Guillevin L, Lhote F, Gayraud M, et al. Prognostic factors in polyarteritis nodosa and Churg-Strauss syndrome. A prospective study in 342 patients. Medicine (Baltimore) 1996;75:17-28.
95. Guillevin L, Lhote F, Gherardi R. Polyarteritis nodosa, microscopic polyangiitis, and Churg-Strauss syndrome: clinical aspects, neurologic manifestations, and treatment. Neurol Clin 1997;15:865-86.
96. Erzurum SC, Underwood GA, Hamilos DL, et al. Pleural effusion in Churg-Strauss syndrome. Chest 1989;95:1357-9.
97. Kim YK, Lee KS, Chung MP, et al. Pulmonary involvement in Churg-Strauss syndrome: an analysis of CT, clinical, and pathologic findings. Eur Radiol 2007;17:3157-65.
98. Primack SL, Miller RR, Muller NL. Diffuse pulmonary hemorrhage: clinical, pathologic, and imaging features. AJR Am J Roentgenol 1995;164:295-300.
99. Leatherman JW, Davies SF, Hoidal JR. Alveolar hemorrhage syndromes: diffuse microvascular lung hemorrhage in immune and idiopathic disorders. Medicine (Baltimore) 1984;63:343-61.
100. Lombard CM, Colby TV, Elliott CG. Surgical pathology of the lung in anti-basement membrane antibody-associated Goodpasture's syndrome. Hum Pathol 1989;20:445-51.
101. Ramos-Casals M, Stone JH, Cid MC, et al. The cryoglobulinaemias. Lancet 2012;379:348-60.
102. Ramos-Casals M, Robles A, Brito-Zeron P, et al. Life-threatening cryoglobulinemia: clinical and immunological characterization of 29 cases. Semin Arthritis Rheum 2006;36:189-96.
103. Amital H, Rubinow A, Naparstek Y. Alveolar hemorrhage in cryoglobulinemia--an indicator of poor prognosis. Clin Exp Rheumatol 2005;23:616-20.
104. Saulsbury FT. Henoch-Schonlein purpura. Curr Opin Rheumatol 2010;22:598-602.
105. Lai FM, Li EK, Suen MW, et al. Pulmonary hemorrhage. A fatal manifestation in IgA nephropathy. Arch Pathol Lab Med 1994;118:542-6.
106. Harland RW, Becker CG, Brandes JC, et al. Immunoglobulin A (IgA) immune complex pneumonitis in a patient with IgA nephropathy. Ann Intern Med 1992;116:220-2.
107. Kathuria S, Cheifec G. Fatal pulmonary Henoch-Schonlein syndrome. Chest 1982;82:654-6.
108. Davis MD, Brewer JD. Urticarial vasculitis and hypocomplementemic urticarial vasculitis syndrome. Immunol Allergy Clin North Am 2004;24:183-213, vi.
109. Schwartz HR, McDuffie FC, Black LF, et al. Hypocomplementemic urticarial vasculitis: association with chronic obstructive pulmonary disease. Mayo Clin Proc 1982;57:231-8.
110. Wisnieski JJ, Baer AN, Christensen J, et al. Hypocomplementemic urticarial vasculitis syndrome. Clinical and serologic findings in 18 patients. Medicine (Baltimore) 1995;74:24-41.
111. Ghamra Z, Stoller JK. Basilar hyperlucency in a patient with emphysema due to hypocomplementemic urticarial vasculitis syndrome. Respir Care 2003;48:697-9.
112. Pujara AC, Mohammed TL. Hypocomplementemic urticarial vasculitis syndrome: a rare cause of basilar panacinar emphysema. J Thorac Imaging 2012;27:W50-1.
113. Davatchi F, Shahram F, Chams-Davatchi C, et al. Behcet's disease: from East to West. Clin Rheumatol

© Cardiovascular Diagnosis and Therapy. All rights reserved.

2010;29:823-33.
114. Criteria for diagnosis of Behcet's disease. International Study Group for Behcet's Disease. Lancet 1990;335:1078-80.
115. Uzun O, Akpolat T, Erkan L. Pulmonary vasculitis in behcet disease: a cumulative analysis. Chest 2005;127:2243-53.
116. Slavin RE, de Groot WJ. Pathology of the lung in Behcet's disease. Case report and review of the literature. Am J Surg Pathol 1981;5:779-88.
117. Erkan F, Gul A, Tasali E. Pulmonary manifestations of Behcet's disease. Thorax 2001;56:572-8.
118. Hamuryudan V, Yurdakul S, Moral F, et al. Pulmonary arterial aneurysms in Behcet's syndrome: a report of 24 cases. Br J Rheumatol 1994;33:48-51.
119. Numan F, Islak C, Berkmen T, et al. Behcet disease: pulmonary arterial involvement in 15 cases. Radiology 1994;192:465-8.
120. Grenier P, Bletry O, Cornud F, et al. Pulmonary involvement in Behcet disease. AJR Am J Roentgenol 1981;137:565-9.
121. Tunaci M, Ozkorkmaz B, Tunaci A, et al. CT findings of pulmonary artery aneurysms during treatment for Behcet's disease. AJR Am J Roentgenol 1999;172:729-33.
122. Gul A, Yilmazbayhan D, Buyukbabani N, et al. Organizing pneumonia associated with pulmonary artery aneurysms in Behcet's disease. Rheumatology (Oxford) 1999;38:1285-9.
123. Berkmen T. MR angiography of aneurysms in Behcet disease: a report of four cases. J Comput Assist Tomogr 1998;22:202-6.
124. Kim WH, Choi D, Kim JS, et al. Effectiveness and safety of endovascular aneurysm treatment in patients with vasculo-Behcet disease. J Endovasc Ther 2009;16:631-6.
125. Mouas H, Lortholary O, Lacombe P, et al. Embolization of multiple pulmonary arterial aneurysms in Behcet's disease. Scand J Rheumatol 1996;25:58-60.
126. Erkan D, Yazici Y, Sanders A, et al. Is Hughes-Stovin syndrome Behcet's disease? Clin Exp Rheumatol 2004;22:S64-8.
127. Specks U. Diffuse alveolar hemorrhage syndromes. Curr Opin Rheumatol 2001;13:12-7.
128. Franks TJ, Koss MN. Pulmonary capillaritis. Curr Opin Pulm Med 2000;6:430-5.
129. Bocanegra TS, Espinoza LR, Vasey FB, et al. Pulmonary hemorrhage in systemic necrotizing vasculitis associated with hepatitis B. Chest 1981;80:102-3.
130. Dykhuizen RS, Smith CC, Kennedy MM, et al. Necrotizing sarcoid granulomatosis with extrapulmonary involvement. Eur Respir J 1997;10:245-7.
131. Zamora MR, Warner ML, Tuder R, et al. Diffuse alveolar hemorrhage and systemic lupus erythematosus. Clinical presentation, histology, survival, and outcome. Medicine (Baltimore) 1997;76:192-202.
132. Miller LR, Greenberg SD, McLarty JW. Lupus lung. Chest 1985;88:265-9.
133. Haupt HM, Moore GW, Hutchins GM. The lung in systemic lupus erythematosus. Analysis of the pathologic changes in 120 patients. Am J Med 1981;71:791-8.
134. Tanaka E, Harigai M, Tanaka M, et al. Pulmonary hypertension in systemic lupus erythematosus: evaluation of clinical characteristics and response to immunosuppressive treatment. J Rheumatol 2002;29:282-7.
135. Schwarz MI, Zamora MR, Hodges TN, et al. Isolated pulmonary capillaritis and diffuse alveolar hemorrhage in rheumatoid arthritis and mixed connective tissue disease. Chest 1998;113:1609-15.
136. Brown I, Joyce C, Hogan PG, et al. Pulmonary vasculitis associated with anti-Jo-1 antibodies. Respir Med 1998;92:986-8.
137. Choi HK, Merkel PA, Walker AM, et al. Drug-associated antineutrophil cytoplasmic antibody-positive vasculitis: prevalence among patients with high titers of antimyeloperoxidase antibodies. Arthritis Rheum 2000;43:405-13.
138. Nicolls MR, Terada LS, Tuder RM, et al. Diffuse alveolar hemorrhage with underlying pulmonary capillaritis in the retinoic acid syndrome. Am J Respir Crit Care Med 1998;158:1302-5.
139. Chung MP, Yi CA, Lee HY, et al. Imaging of pulmonary vasculitis. Radiology 2010;255:322-41.
140. Jamadar DA, Kazerooni EA, Daly BD, et al. Pulmonary zygomycosis: CT appearance. J Comput Assist Tomogr 1995;19:733-8.
141. Travis WD, Pittaluga S, Lipschik GY, et al. Atypical pathologic manifestations of Pneumocystis carinii pneumonia in the acquired immune deficiency syndrome. Review of 123 lung biopsies from 76 patients with emphasis on cysts, vascular invasion, vasculitis, and granulomas. Am J Surg Pathol 1990;14:615-25.

Cite this article as: Batra K, Chamarthy M, Chate RC, Jordan K, Kay FU. Pulmonary vasculitis: diagnosis and endovascular therapy. Cardiovasc Diagn Ther 2018;8(3):297-315. doi: 10.21037/cdt.2017.12.06

© Cardiovascular Diagnosis and Therapy. All rights reserved.